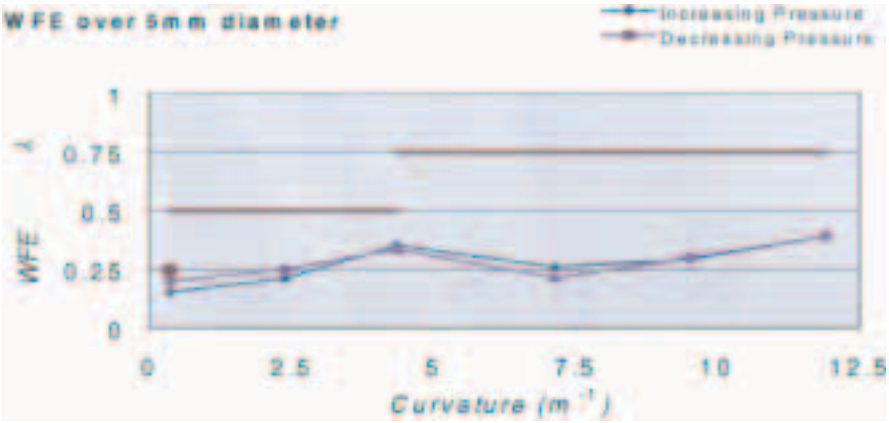

Figure 2: VCM optical surface quality over a 5-mm diameter. The wavefront error (WFE) is given as a peak-to-valley (PTV) in fraction of λ.

Figure 2 presents the optical quality (PTV) achieved with one of the VCM mirrors on the whole curvature range, compared to the required performances.

On the central part of the VCM, 5 mm diameter, analysis shows that the deviation from a sphere remains below λ/2 ptv during the whole curvature range (2800–84 mm).

Curvature Control Accuracy

The other important point, related to the pupil positioning in the interferometric laboratory, is the adjustment of a precise curvature during the operation of the VCMs.

In order to achieve a precise curvature, the air pressure on the back side of the mirror is controlled on open loop with a 5.10^{-4} accuracy in the 0–10 bar range. This high accuracy on the pressure control has been combined with an "hysteresis" model for the meniscus deformation. The effect is present only during the phase of decreasing pressure and depends on the maximum pressure reached during the cycle.

The model allows to take into account the history of the mirror and computes the right pressure to achieve the required curvature. An output of the model is presented in Figure 3 where ΔP is the correction to be applied (to correct for the hysteresis effect) as a function of the maximum pressure reached during the cycle.

Using the high-accuracy pressure control and the hysteresis model, the resulting error on the VCM curvature is less than 5.10^{-3} m^{-1} and leads to a 15-cm pupil position accuracy in the interferometric laboratory.

The error on the pupil position will be reduced by the beam compressor system, located at the entrance of the laboratory, to less than 1 cm at the instruments entrance and this value has to be compared with the 70 metres stroke of the delay line carriage.

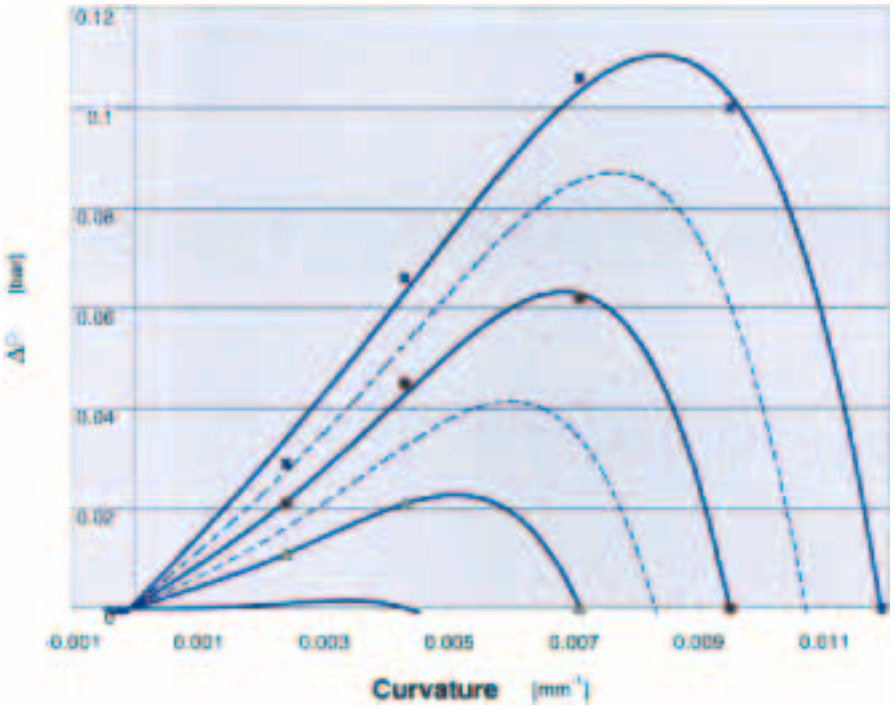

Figure 3: Correction to be applied to correct for the hysteresis effect. The lines represent the hysteresis model and the dots the measured values for various maximal pressures reached during a cycle.

Conclusion

This is not the first time that such an optical device, a varifocal mirror, has been achieved. But this one, thanks to the expertise of the team in Marseille Observatory, has an exceptionally wide range of curvature combined with a very good optical quality and a high curvature accuracy. This will allow the VLTI to deliver a good entrance pupil to the interferometric instruments.

Today this VCM has been delivered to ESO and is being included in the delay lines in order to set up and calibrate the interfaces with the other devices of the interferometric mode. The integration will be done during this year, the first complete systems (delay lines with VCMs) will be installed on Paranal during the year 2000.

The VLTI Test Siderostats Are Ready for First Light

F. DERIE, E. BRUNETTO and M. FERRARI, ESO

To allow the technical commissioning of the VLTI in its early phases, without the VLT Unit Telescopes or the Auxiliary Telescopes, two test siderostats have been developed to simulate the main functions and interfaces of these telescopes.

The principal objective of the optical concept (Fig. 1) of the siderostat is to optimise the collecting area over a sky coverage defined by the scientific targets chosen for the commissioning of the VLTI with the test instrument VINCI and the IR instrument MIDI. The diameter of the 400-mm free aperture of the Alt-Azimuth siderostat has been chosen to allow the observation in the N Band of all MIDI targets (Table 1). The angles between the different mirrors are optimised for the latitude of Paranal. To simulate the 80-mm diameter pupil size of a Unit Telescope,

Figure 1: Three-dimensional representation of the VLTI Test-Siderostat Optical Path. The diameter of the Siderostat mirror is 400 mm and the second plane mirror (upper part of the periscope) is at 25° angle of elevation. The use of a Beam Compressor allows to have an 80-mm output pupil (similar to the ones of the Unit Telescopes).

a beam compressor (5:1) is introduced between the Siderostat mirrors. The development of the beam compressor is made in collaboration with MPIA Heidelberg. The output pupil shape is, as expected by principle of a siderostat, an ellipse whose size and orientation vary in function of the direction of observation (Fig. 2). The small circle in the centre (at 0.0, 0.0 space Zenith position) represents the full aperture of the siderostat mirror. Field rotation due to Alt-Azimuth siderostat movement (bottom part of the figure) and vignetting due to the relay optics (central upper part) can be clearly identified.

Based not only on dedicated requirements for the optics, mechanics and control, but also on the above optical design and on the site interface, the development of two siderostats has been contracted to Halfmann Teleskoptechnik GmbH located at Neusäß near Augsburg. The detail design and the manufacture were achieved in less than one year. Figure 3, taken during the last assembly, shows the system ready for alignment tests prior to packing and delivery to Paranal. The five mirrors have an optical quality better than 25 nm RMS and are gold coated. The full structure is made of steel that preserves high rigidity. The dimensions are about 2.5 m in height and 2.2 m in diameter at the level of the yellow frame. Only the upper part will be visible above Paranal ground. The frame and the lower part will be located inside the AT station pier to have the output beam exactly at the level of the delay line entrance. With a weight of about 1.75 tons, the complete structure will be easily transported with a crane to allow, as requested during commissioning, relocation of the siderostat between AT stations. For this purpose a minimum of 8 stations will be equipped with a dedicated anchoring system.

Figure 3.

The functions of pointing and tracking are realised by a control system coupled to a CCD camera. The CCD is located at the focus of a guiding scope.

In the background of the picture one can see the two enclosures ready for packing. For these enclosures it was decided to re-use the same concept as for the Astronomical Seeing Monitor (ASM) that has been used for two years at Paranal. Taking advantage of the ASM experience, few modifications have been retrofitted to the design of the siderostat enclosure. What is not shown on the picture is the electrical cabinet that holds the control system. This cabinet will be located a few metres away from the enclosure.

Some performance tests have been carried out during the last weeks with good results. But, the fine-pointing per-

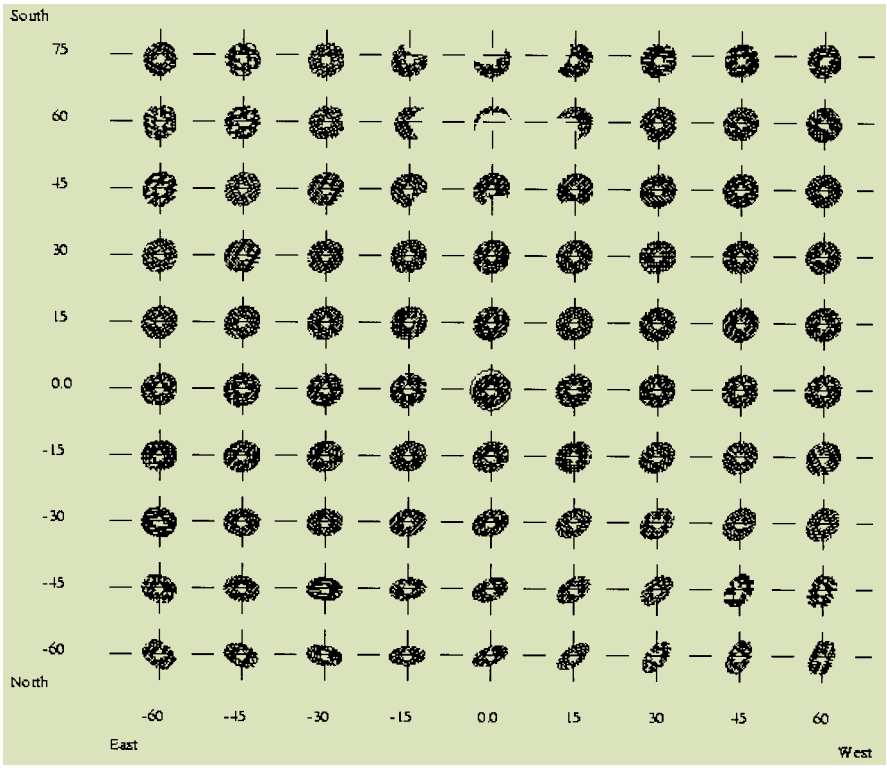

Figure 2.: Output pupil shape as a function of the direction of observation.

formance is still to be measured when good weather conditions will allow us to observe a star in the sky of Neusäß.

With an optical design optimised for the targets of the technical commissioning of the VLTI and its instruments, with high-quality optics, high rigidity of the mechanics and good control electronics, the two siderostats to be installed early 2000 will offer the capability to characterise the VLTI in its first phase. As done for the Astronomical Seeing Monitor, it is envisaged to upgrade the CCD camera by a VLT technical CCD and to perform the necessary upgrade of the control electronics and software to fully meet the ESO VLT standard.

Table 1: List of sources bright enough to be used with 400-mm diameter siderostats (C means N magnitude corresponding to correlated flux).

#	Object	1950 Coordinates	Magnitudes	
1	Alfa Ori	52 27.8 +07 23 58:	V=0.5	C=–4.5
2	Alfa Sco	26 17.9 –26 19 19:	V=1.0	C=–4.0
3	Alfa Tau	33 03.0 +16 24 30:	V=1.5	C=–3.0
4	L2 Pup	12 01.8 –44 33 17:	V=5.1	C=–3.0
5	R Leo	44 52.1 +11 39 41:	V=6.0	C=–3.0
6	IRC + 10 216	45 14.2 +13 30 40:		C=–3.0
7	V766 Cen	43 40.3 –62 20 25:	V=6.5	C=–3.0
8	Alfa Her	12 21.6 +14 26 46:	V=3.5	C=–3.0
9	VX Sgr	05 02.5 –22 13 56:		C=–3.2
10	R Aqr	41 14.1 –15 33 46:	V=6.4	C=–3.1

Myopic Deconvolution of Adaptive Optics Images

J.C. CHRISTOU[1], D. BONACCINI[2], N. AGEORGES[2], and F. MARCHIS[3]

[1]US Air Force Research Laboratory, Kirtland AFB, New Mexico, USA (christou@as.arizona.edu)
[2]ESO, Garching bei München, Germany (dbonacci@eso.org, nageorge@eso.org)
[3]ESO, Santiago, Chile (fmarchis@eso.org)

Abstract

Adaptive Optics produces diffraction-limited images, always leaving a residual uncorrected image and sometime PSF artifacts due, e.g., to the deformable mirror. Post-processing is in some cases necessary to complete the correction and fully restore the image. The results of applying a multi-frame iterative deconvolution algorithm to simulated and actual Adaptive Optics data are presented, showing examples of the application and demonstrating the usefulness of the technique in Adaptive Optics image post-processing. The advantage of the algorithm is that the frame-to-frame variability of the PSF is beneficial to its convergence, and the partial knowledge of the calibrated PSF during the observations is fully exploited for the convergence. The analysis considers the aspects of morphology, astrometry, photometry and the effect of noise in the images. Point sources and extended objects are considered.

1. Introduction

This paper reports on work done to establish and evaluate data reduction procedures specifically applicable to Adaptive Optics (AO) data. The programme evaluated for multi-frame iterative blind deconvolution, IDAC, is provided by J. Christou and available in the ESO Web page at `http://www.ls.eso.org/lasilla/Telescope/360cat/adonis/html/datared.html#distrib` for the Unix platforms.

This work is part of a dedicated effort to guide the AO users in the data reduction process and to produce specific data-reduction tools. The observing data presented here were taken with Adonis at the La Silla 3.6-m telescope during technical time, specifically dedicated to this data-reduction programme.

Adaptive Optics (AO) is now a proven technology for real-time compensation of space objects, to remove the degrading effects of the Earth's atmosphere. However, the compensation is never "perfect" and residual wavefront errors remain, which in some cases can lead to significant uncompensated power. This decreases the image contrast making, in some cases, necessary to use some form of image post-processing to remove the effects of the system's point spread function (PSF). The knowledge of good deconvolution techniques suitable on AO images is also important to boost images with low Strehl, e.g. from low-order AO systems.

AO compensation is achieved via a servo-control loop which uses a reference signal from a guide star (GS) to zero the wavefront error at each iteration, typically every 2–40 msec chosen depending on the observing wavelength and reference signal strength. It is well known that the performance of an AO system is limited by the reference signal strength as well as by the atmospheric coherence length r_0, the atmospheric coherence time to, and the isoplanatic angle θ_0.

In astronomical imaging, exposure times from a few msec to tens of minutes are used. The variability of r_0 and of the AO PSF can be quite large in short integration times (seconds), while it smoothes out in timescales of minutes. There is also a slow decline in Strehl Ratio (SR), the system's performance parameter[1], across an imaging field of radius θ_0 due to field anisoplanatism effect. The latter produces mainly an elongation of the PSF in the direction of the GS, which is function of the object radial distance. The PSF at the reference star has a diffraction-limited core, surrounded by a broad gaussian halo.

Static and dynamic artifacts in the image due to either print-through of the deformable mirror actuators, and differential aberrations between the science and WFS optical paths, have also been observed. For ADONIS, the former have a Gaussian shape with peak intensities in the range of 0.5% to 1% of the central PSF core. Although their energy content is undoubtedly small, if not removed they make it difficult to unambiguously identify faint objects or faint structures around bright sources.

Thus the observer has to worry about time-varying and space-varying AO PSFs.

In general, the observation of a point source as PSF Calibrator, in addition to the target, is used to further improve the compensated image via post-processing. However, the AO compensation obtained on the target and the PSF calibrator are not necessarily the same: the

[1]The Strehl Ratio is a standard measure for the performance of an AO system. It is the ratio of the maximum intensity of the delivered PSF to the maximum of the theoretical diffraction-limited PSF when both PSFs are normalised to unity. A Strehl Ratio of 1 means achievement of the theoretically best performance.